



## King's Research Portal

DOI:

[10.1016/j.omtm.2018.07.012](https://doi.org/10.1016/j.omtm.2018.07.012)

*Document Version*

Peer reviewed version

[Link to publication record in King's Research Portal](#)

*Citation for published version (APA):*

Weber, L., Poletti, V., Magrin, E., Antoniani, C., Martin, S., Bayard, C., ... Miccio, A. (2018). An optimized lentiviral vector corrects efficiently the human sickle cell disease phenotype. *Molecular Therapy - Methods and Clinical Development*. <https://doi.org/10.1016/j.omtm.2018.07.012>

### **Citing this paper**

Please note that where the full-text provided on King's Research Portal is the Author Accepted Manuscript or Post-Print version this may differ from the final Published version. If citing, it is advised that you check and use the publisher's definitive version for pagination, volume/issue, and date of publication details. And where the final published version is provided on the Research Portal, if citing you are again advised to check the publisher's website for any subsequent corrections.

### **General rights**

Copyright and moral rights for the publications made accessible in the Research Portal are retained by the authors and/or other copyright owners and it is a condition of accessing publications that users recognize and abide by the legal requirements associated with these rights.

- Users may download and print one copy of any publication from the Research Portal for the purpose of private study or research.
- You may not further distribute the material or use it for any profit-making activity or commercial gain
- You may freely distribute the URL identifying the publication in the Research Portal

### **Take down policy**

If you believe that this document breaches copyright please contact [librarypure@kcl.ac.uk](mailto:librarypure@kcl.ac.uk) providing details, and we will remove access to the work immediately and investigate your claim.

# Accepted Manuscript

An optimized lentiviral vector corrects efficiently the human sickle cell disease phenotype

Leslie Weber, Valentina Poletti, Elisa Magrin, Chiara Antoniani, Samia Martin, Charles Bayard, Hanem Sadek, Tristan Felix, Vasco Meneghini, Michael N. Antoniou, Wassim El- Nemer, Fulvio Mavilio, Marina Cavazzana, Isabelle Andre-Schmutz, Annarita Miccio

PII: S2329-0501(18)30076-7

DOI: [10.1016/j.omtm.2018.07.012](https://doi.org/10.1016/j.omtm.2018.07.012)

Reference: OMTM 167

To appear in: *Molecular Therapy: Methods & Clinical Development*

Received Date: 26 June 2018

Accepted Date: 29 July 2018

Please cite this article as: Weber L, Poletti V, Magrin E, Antoniani C, Martin S, Bayard C, Sadek H, Felix T, Meneghini V, Antoniou MN, El- Nemer W, Mavilio F, Cavazzana M, Andre-Schmutz I, Miccio A, An optimized lentiviral vector corrects efficiently the human sickle cell disease phenotype, *Molecular Therapy: Methods & Clinical Development* (2018), doi: 10.1016/j.omtm.2018.07.012.

This is a PDF file of an unedited manuscript that has been accepted for publication. As a service to our customers we are providing this early version of the manuscript. The manuscript will undergo copyediting, typesetting, and review of the resulting proof before it is published in its final form. Please note that during the production process errors may be discovered which could affect the content, and all legal disclaimers that apply to the journal pertain.



**An optimized lentiviral vector corrects efficiently the human sickle cell disease phenotype**

Leslie Weber<sup>1,2</sup>, Valentina Poletti<sup>3</sup>, Elisa Magrin<sup>4</sup>, Chiara Antoniani<sup>5,6</sup>, Samia Martin<sup>3</sup>, Charles Bayard<sup>1</sup>, Hanem Sadek<sup>1</sup>, Tristan Felix<sup>5,6</sup>, Vasco Meneghini<sup>5,6</sup>, Michael N Antoniou<sup>7</sup>, Wassim El- Nemer<sup>8,9,10</sup>, Fulvio Mavilio<sup>5,11</sup>, Marina Cavazzana<sup>1,4,5</sup>, Isabelle Andre-Schmutz<sup>1,5</sup> and Annarita Miccio<sup>3,5,6</sup>

<sup>1</sup>Laboratory of Human Lymphohematopoiesis, INSERM UMR\_S1163, 75015 Paris, France

<sup>2</sup>Paris Diderot University – Sorbonne Paris Cité, 75015 Paris, France

<sup>3</sup>Genethon, INSERM UMR951, 91000 Evry, France

<sup>4</sup>Biotherapy Department, Necker Children's Hospital, Assistance Publique-Hôpitaux de Paris, 75015 Paris, France

<sup>5</sup>Paris Descartes–Sorbonne Paris Cité University, Imagine Institute, 75015 Paris, France

<sup>6</sup>Laboratory of chromatin and gene regulation during development, INSERM UMR\_S1163, 75015 Paris, France

<sup>7</sup>King's College London, WC2R 2LS London, England

<sup>8</sup>Biologie Intégrée du Globule Rouge, INSERM UMR\_S1134, Paris Diderot University, Sorbonne Paris Cité, Univ. de la Réunion, Univ. des Antilles, 75015 Paris, France

<sup>9</sup>Institut National de la Transfusion Sanguine, 75015 Paris, France

<sup>10</sup>Laboratoire d'Excellence GR-Ex, 75015 Paris, France

<sup>11</sup>Department of Life Sciences, University of Modena and Reggio Emilia, 41125 Modena, Italy

Correspondence should be addressed to A.M., Imagine Institute, 24, Boulevard du Montparnasse, 75015 Paris, France. E-mail address: annarita.miccio@institutimagine.org.

Running title: Lentiviral-based gene therapy for Sickle Cell Disease

**ABSTRACT**

Autologous transplantation of hematopoietic stem cells transduced with a lentiviral vector (LV) expressing an anti-sickling *HBB* variant is a potential treatment for sickle cell disease (SCD). With a clinical trial as our ultimate goal, we generated LV constructs containing an anti-sickling *HBB* transgene (*HBBAS3*), a minimal *HBB* promoter and different combinations of DNase I hypersensitive sites (HSs) from the locus control region (LCR). Hematopoietic stem progenitor cells (HSPCs) from SCD patients were transduced with LVs containing either HS2 and HS3 ( $\beta$ -AS3) or HS2, HS3 and HS4 ( $\beta$ -AS3 HS4). The inclusion of the HS4 element drastically reduced vector titer and infectivity in HSPCs, with negligible improvement of transgene expression. Conversely, the LV containing only HS2 and HS3 was able to efficiently transduce SCD bone marrow and Plerixafor-mobilized HSPCs, with anti-sickling HBB representing up to ~60% of the total HBB-like chains. The expression of the anti-sickling HBB and the reduced incorporation of the  $\beta^S$ -chain in hemoglobin tetramers allowed up to 50% reduction in the frequency of RBC sickling under hypoxic conditions. Together these results demonstrate the ability of a high titer LV to express elevated levels of a potent anti-sickling *HBB* transgene ameliorating the SCD cell phenotype.

## INTRODUCTION

Sickle cell disease (SCD) is a severe genetic disorder affecting ~312,000 newborns worldwide annually.<sup>1</sup> A single point mutation in the adult  $\beta$ -globin (*HBB*) gene causes a Glu>Val amino acid substitution in the  $\beta$ -globin chain ( $\beta^S$ -globin). The sickle hemoglobin (HbS,  $\alpha_2\beta^S_2$ ) has the propensity to polymerize under deoxygenated conditions, resulting in the production of sickle-shaped red blood cells (RBCs) that can cause occlusions of blood vessels, leading to impaired oxygen delivery to tissues, respiratory complications, organ damage and early mortality. Additionally, sickled RBCs are prone to hemolysis, thus the clinical phenotype is also characterized by hemolytic anemia. Current treatments include life-long RBC transfusions and hydroxyurea, a drug that increases fetal Hb (HbF,  $\alpha_2\gamma_2$ ) synthesis<sup>2</sup>. Indeed, the clinical course of SCD is improved when fetal *HBB* genes are highly expressed, as seen in patients with naturally occurring mutations leading to hereditary persistence of fetal hemoglobin (HPFH). In SCD, HbF exerts a potent anti-sickling function by competing with the sickle  $\beta^S$ -globin for incorporation in Hb tetramers and by inhibiting HbS polymerization. However, pharmacological treatments increasing HbF levels are not equally effective in all patients.<sup>2</sup>

The only definitive cure for SCD patients is allogeneic hematopoietic stem cell (HSC) transplantation. However, HSC transplantation from an HLA-matched related donor is available only to a fraction of patients.<sup>3</sup> Transplantation of HSCs from matched unrelated donors are associated with a higher risk of graft-versus-host-disease, transplant rejection and infections<sup>3</sup>. With the advent of *HBB* expressing lentiviral vectors (LVs), transplantation of genetically modified autologous HSCs holds promise of circumventing the need for suitable donors and the morbidity and mortality associated with allogeneic transplantation.

LV-based *ex vivo* gene therapy strategies require the stable transfer of an anti-sickling

*HBB* globin transgene in the patient's long-term repopulating HSCs and high, sustained and regulated expression of the therapeutic globin chain in their erythroid progeny. Several LVs have been developed and tested in murine models of SCD and patient hematopoietic stem progenitor cells (HSPCs).<sup>4-6</sup> In these vectors, an anti-sickling *HBB* transgene (*HBG* or  $\beta^{\text{T87Q}}$  and  $\beta^{\text{AS3}}$  *HBB* anti-sickling variants) is placed under the transcriptional control of the *HBB* promoter and key regulatory elements from the 16-kb human  $\beta$ -locus control region ( $\beta$ LCR), which is essential for high and regulated expression of the endogenous *HBB* gene family.<sup>7</sup> Since LVs cannot accommodate the entire LCR, only the 3 most transcriptionally potent out of the 5 DNase I hypersensitive sites (HS2, HS3 and HS4) were selected and reduced in size to fit into the vector packaging capacity. The combination of minimal core elements of HS2, HS3 and HS4 (each of them 0.2 to 0.4 kb-long) was associated with low transgene expression levels, positional variegation and transcriptional silencing, whereas extended HSs sustained high *HBB*-like globin expression.<sup>8, 9</sup> Sequences flanking the HS core elements might indeed be required for synergistic activation of *HBB*-like globin gene expression.<sup>10</sup> Therefore, *HBB* globin expressing LVs are exceptionally large, harboring a 2.6- to 3.4-kb "mini-LCR" containing extended HS2, HS3 and HS4.<sup>4-6</sup> The large size of these vectors makes their production challenging and might affect gene transfer efficiency, particularly in HSPCs.<sup>8</sup>

There have been three clinical trials for SCD using LVs expressing an anti-sickling *HBB*-like globin gene (see <sup>11, 12</sup>). The first SCD patient to have undergone gene therapy showed a good correction of the clinical phenotype and the biological hallmarks of SCD.<sup>13</sup> However, in a parallel study using the same LV, gene marking in the peripheral blood was low in all treated SCD subjects, with no evidence of clinical benefit.<sup>14</sup> Therefore, the development of high-titer LVs able to transduce a good proportion of HSCs and drive high levels of *HBB*-like expression is still a critical issue to achieve therapeutic efficacy in SCD patients. In particular, the choice of  $\beta$ LCR regulatory elements able to drive high levels of

*HBB*-like expression without compromising the vector titer is critical.

Here, we show that a compact, high titer LV, containing only the HS2 and HS3  $\beta$ LCR elements, is highly efficient in transducing a large proportion of SCD HSPCs derived from bone marrow or mobilized in the peripheral blood of SCD patients, and expressed therapeutic levels of a potent anti-sickling *HBB* transgene.

## RESULTS

### Design and characterization of lentiviral vectors expressing an anti-sickling human *HBB* transgene

We generated two LVs carrying an anti-sickling human *HBB* transgene (*HBBAS3*) under the transcriptional control of a minimal *HBB* promoter and either two or three HSs from the human  $\beta$ LCR: HS2 and HS3 ( $\beta$ -AS3 LV) and HS2, HS3 and HS4 ( $\beta$ -AS3 HS4 LV)) (**Figure 1A**). The *HBBAS3* gene contains three mutations<sup>15</sup> causing three potentially beneficial “anti-sickling” amino-acidic substitutions (G16D, E22A, T87Q) in the LV-derived HBB chain ( $\beta^{\text{AS3}}$ ): A22 and Q87 impair respectively the axial and lateral contacts necessary for the formation of HbS polymers, and D16 increases the affinity to HBA chains, thus conferring to  $\beta^{\text{AS3}}$  a competitive advantage for the incorporation in the Hb tetramers<sup>15</sup> (**Figure 1A**).

VSV-G pseudotyped, third generation LVs were produced by standard transient transfection of HEK293T cells and concentrated by ultra-centrifugation. The physical titer of the two vectors, determined by measuring the viral p24 protein, was similar, indicating that a comparable amount of total viral particles was present in the  $\beta$ -AS3 LV and  $\beta$ -AS3 HS4 vector preparations (**Figure 1B**). We then transduced HCT116 cells and human erythroid (HEL and K562) cell lines to determine the infectious titer by measuring the average number

of vector copies integrated per genome (vector copy number; VCN). The infectious titer of  $\beta$ -AS3 LV was ~8-fold higher, compared to  $\beta$ -AS3 HS4 LV (**Figure 1B**). As a consequence,  $\beta$ -AS3 LV showed a markedly increased infectivity, measured as ratio between the infectious and the physical titer (**Figure 1B**). We then transduced human G-CSF-mobilized peripheral blood (mPB) HSPCs from healthy donors (HD) with increasing amounts of vector preparations. Notably,  $\beta$ -AS3 LV showed a superior gene transfer efficiency compared to  $\beta$ -AS3 HS4, leading to up to  $2.40 \pm 0.58$  vector copies per cell at the highest vector dose (**Figure 1C**).

Given these results, we next investigated the potential detrimental effects of the HS4 element on viral titer and infectivity. Total RNA was extracted from HEK293T packaging cells transfected with  $\beta$ -AS3 and  $\beta$ -AS3 HS4 transfer vectors and LV packaging plasmids. RT-qPCR analysis revealed that the total viral genomic RNA containing the  $\psi^+$  packaging signal was significantly higher for  $\beta$ -AS3 LV compared to the HS4-containing LV (**Figure 1D**). In addition, by using 3' RACE-PCR, followed by Sanger sequencing, we detected a truncated  $\beta$ -AS3 HS4 viral genomic transcript (**Figure S1A**). We identified a canonical polyadenylation signal (AATAAA) in the HS4 element, likely responsible of the premature truncation of the  $\beta$ -AS3 HS4 viral transcripts (**Figure S1A**). However, RT-qPCR showed a comparable fraction of full length viral RNA (~20% of the total  $\psi^+$  viral genomic RNA) for both  $\beta$ -AS3 and  $\beta$ -AS3 HS4 LVs (**Figure S1B**).

To understand the reasons for the significant drop in titer cause by the 1.1-kb long HS4, we constructed the  $\beta$ -AS3 HS4 core LV harboring a short 304-bp HS4 fragment containing the core HS4 element<sup>10</sup> and lacking the polyadenylation site mapped in the long HS4 element. (**Figure S1C**). Although the shortening of the HS4 element restored most of the total  $\psi^+$  viral genomic RNA levels, it did not increase significantly the infectious titer and infectivity in



HCT116 cells, thus indicating that even the core HS4 element contain sequences that are detrimental to the vector performance (**Figure S1D and E**).

### **$\beta$ -AS3 transduction leads to highly efficient gene transfer in SCD bone marrow HSPC**

In order to evaluate gene transfer efficiency of the  $\beta$ -AS3 and  $\beta$ -AS3 HS4 LVs, we transduced SCD patient bone marrow (BM) HSPCs samples with an equal number of infecting particles (multiplicity of infection [MOI] 4 to 360; n=2-6; 2 donors). HSPCs were either differentiated in liquid culture towards the erythroid lineage or plated in semi-solid medium containing cytokines supporting the clonal growth and differentiation of erythroid (BFU-E) and granulocyte-monocyte (CFU-GM) progenitors (Colony Forming Cell (CFC) assay). Lentiviral transduction did not affect erythroid proliferation and differentiation, and clonogenic potential of transduced HSPCs (**Figure S2, Figure 2A and data not shown**).

Negligible gene transfer efficiency was observed using  $\beta$ -AS3 HS4 with a MOI lower than 36 (data not shown). HSPC transduction with  $\beta$ -AS3 HS4 at an MOI of 36 led to the integration of  $0.55\pm0.41$ ,  $0.70\pm0.31$  and  $0.43\pm0.23$  vector copies per cell in erythroblasts, and pools of BFU-E and CFU-GM, respectively. A 10-fold increase in  $\beta$ -AS3 HS4 infecting particles did not increase the gene transfer efficiency (**Figure 2B**). In contrast,  $\beta$ -AS3 was able to transduce HSPCs even at low MOIs (4- and 12; **Figure 2B**). The VCN of  $\beta$ -AS3 was positively correlated with the MOIs, rising up to  $4.81\pm1.29$  in erythroblasts,  $4.13\pm0.95$  in BFU-E and  $1.49\pm0.67$  in CFU-GM at an MOI of 360. Notably, at the same MOIs  $\beta$ -AS3 transduction efficiency was significantly higher, as compared to  $\beta$ -AS3 HS4 (**Figure 2B**).

To assess precisely the frequency of transduced HSPCs, we measured the gene transfer efficiency in individual BFU-E and CFU-GM (n=3-6; 2 donors). When HSPCs were transduced using the same vector doses, a higher proportion of transduced CFCs was

observed for  $\beta$ -AS3 compared to  $\beta$ -AS3 HS4 (**Figure 2C**). We observed up to 82% and 67% of  $\beta$ -AS3-transduced BFU-E and CFU-GM, respectively. In contrast,  $\beta$ -AS3 HS4 did not transduce  $>40\%$  of CFCs (**Figure 2C**). Samples containing  $<40\%$  of transduced CFCs (e.g.  $\beta$ -AS3 HS4 MOI 360 and 36 and  $\beta$ -AS3 MOI 4 and 12) displayed a similar VCN distribution, with most of the transduced BFU-E and CFU-GM harboring 1 to 2 vector copies per genome. Notably, the high frequency of transduction reached using  $\beta$ -AS3 at the highest doses (e.g. MOI 36 and 360) was accompanied with a significantly higher proportion of progenitors harboring  $>3$  vector copies per cell (from 10 to 65%), compared to  $\beta$ -AS3 HS4 ( $<5\%$ ) (**Figure 2D**).

### **$\beta$ -AS3 outperforms $\beta$ -AS3 HS4 in the transduction of long-term repopulating HSCs**

We then compared gene transfer efficiency of the  $\beta$ -AS3 HS4 and  $\beta$ -AS3 LVs in long-term repopulating SCD HSCs. BM-derived HSPCs from a SCD patient were transduced at an MOI of 360 and injected into NSG immunodeficient mice after busulfan-based conditioning (n=5 mice per vector). As expected, the transduction efficiency of the input SCD HSPC populations was higher for  $\beta$ -AS3 than for  $\beta$ -AS3 HS4, as assessed *in vitro* in BFU-E and CFU-GM pools (0.26 and 0.18  $\beta$ -AS3 HS4 vector copies in BFU-E and CFU-GM; 2.03 and 0.66  $\beta$ -AS3 vector copies in BFU-E and CFU-GM). As controls, we transplanted mock-transduced SCD HSPCs (n=5 mice) and adult G-CSF-mobilized peripheral blood (mPB) or cord blood (CB) HSPCs obtained from healthy donors (HD) (n=5 mice).

Mice were euthanized and hematopoietic organs were analyzed for the engraftment of human cells, calculated as percentage of human CD45<sup>+</sup> cells in the total human and murine CD45<sup>+</sup> cell populations. The engraftment was similar among mock and transduced conditions in BM, spleen and thymus (**Figures 3A**). Comparable frequencies were observed upon

transplantation of healthy donor HSPCs, except for a higher engraftment of human CD45<sup>+</sup> cells in the spleen and thymus of mice transplanted with CB-derived HSPCs. We detected a similar distribution of B, T and myeloid cells in the CD45<sup>+</sup> cell populations across the different conditions (**Figure S3**).

Total BM cells were isolated and subjected to a CFC assay to assess the gene transfer efficiency in HSC-derived BFU-E and CFU-GM pools. Clonogenic potential was similar between mock and transduced samples (**Figure 3B**). The average  $\beta$ -AS3 HS4 VCN per cell was  $0.04 \pm 0.001$  in BFU-E and  $0.02 \pm 0.001$  in CFU-GM, whereas the  $\beta$ -AS3-transduced CFCs displayed a significantly higher VCN/cell ( $0.34 \pm 0.12$  in BFU-E and of  $0.23 \pm 0.08$  in CFU-GM; **Figure 3C**).

Taken together, these results confirmed the superior gene transfer efficiency of the  $\beta$ -AS3 vector in long-term repopulating HSCs compared to the  $\beta$ -AS3 HS4 LV harboring an additional  $\beta$ LCR HS site.

### **$\beta$ -AS3 LV-derived transgene expression ameliorates the SCD cell phenotype *in vitro***

To compare the therapeutic potential of the  $\beta$ -AS3 and  $\beta$ -AS3 HS4 LVs in terms of transgene expression and correction of the SCD phenotype, we differentiated *in vitro* transduced SCD BM HSPCs into mature RBCs (n=3-4; 2 donors). Erythroid differentiation was monitored over time by flow cytometry and morphological analyses. Downregulation of early erythroid markers CD36 and CD71 and upregulation of the late erythroid marker glycophorin A (GYPA) occurred similarly in mock and transduced samples (**Figure S2A and 2B**). RBC enucleation was obtained at day-20 post differentiation for all the samples, as demonstrated by the loss of cells staining with the nuclear dye DRAQ5 and by morphological analyses (**Figure S2A, S2B and S2C**).

*HBBAS3* transgene mRNA expression was measured by RT-qPCR in erythroblasts derived from  $\beta$ -AS3- and  $\beta$ -AS3 HS4-transduced HSPCs. We observed a strong correlation between transgene expression and average VCN for both  $\beta$ -AS3 HS4 and  $\beta$ -AS3 LVs (Pearson correlation  $r=0.99$ ,  $P<0.0001$ , **Figure 4A**). Despite the lack of the HS4 element in the  $\beta$ -AS3 construct, no statistically significant differences in *HBBAS3* expression were observed between the two vectors in erythroblasts derived from HSPCs harboring a similar VCN (**Figure 4A**). Given the higher transduction efficiency,  $\beta$ -AS3 LV-derived *HBBAS3* expression was overall higher in erythroblasts derived from SCD HSPCs transduced at high MOIs (e.g. 36 and 360), as compared to  $\beta$ -AS3 HS4-transduced samples ( $\beta$ -AS3 mRNA levels:  $0.37\pm0.11$  and  $0.09\pm0.03$ , respectively). Similar results were obtained in BFU-E transduced with  $\beta$ -AS3 HS4 and  $\beta$ -AS3 LVs (**Figure S4A**).

The expression of the Hb tetramer containing the therapeutic  $\beta^{\text{AS3}}$ globin-chain (HbAS3) was detected in mature RBCs by HPLC and was accompanied by a reduction in the levels of HbS containing  $\beta^{\text{S}}$ -chains (**Figure 4B and 4C**). HbAS3 expression was positively correlated with the VCN/cell of  $\beta$ -AS3 HS4 and  $\beta$ -AS3 LVs (Pearson correlation  $r=0.94$ ,  $P<0.0001$  for  $\beta$ -AS3 and  $r=1$ ,  $P<0.001$  for  $\beta$ -AS3 HS4, **Figure 4B**). We observed no significant differences in HbAS3 content in RBCs derived from HSPCs harboring similar  $\beta$ -AS3 HS4 and  $\beta$ -AS3 vector copies (**Figure 4B and C**). Indeed, HbAS3 expression normalized per VCN was similar for the 2 vectors (**Figure 4B**). Notably, HSPC transduction with the  $\beta$ -AS3 LV led to greater protein expression at MOIs higher than 36 compared to  $\beta$ -AS3 HS4 ( $39.26\%\pm6.92\%$  for  $\beta$ -AS3 and  $14.87\%\pm4.09\%$  for  $\beta$ -AS3 HS4;  $P<0.05$ ). Similarly, no differences in HbAS3 expression were observed in BFU-E harboring similar  $\beta$ -AS3 HS4 and  $\beta$ -AS3 VCNs (**Figure S4B**).

The high levels of  $\beta$ -AS3-derived anti-sickling transgene expression prompted us to assess the ability of  $\beta$ -AS3 LV to correct the SCD cell phenotype. To measure the frequency

of sickling and corrected RBCs, we performed an *in vitro* sickling assay under hypoxic conditions. SCD BM HSPCs were transduced with increasing  $\beta$ -AS3 vector doses and differentiated in mature RBCs (n=2 donors). Upon deoxygenation, the frequency of sickling RBCs was >80% in mock-transduced samples (**Figure 4D**). In marked contrast, HSPC transduction with the  $\beta$ -AS3 LV led to a decreased frequency of sickling RBCs and to significant proportions of biconcave RBCs under 0% O<sub>2</sub> (**Figure 4D**). The percentage of corrected (i.e. non-sickling) RBCs increased gradually with the VCN, reaching 34% and 47% of corrected RBCs for donor 1 and 2, respectively (**Figure 4E**). Notably, the extent of the RBC correction was positively correlated with the HbAS3 production (**Figure 4F**).

#### **$\beta$ -AS3 LV efficiently transduces SCD mobilized HSPCs**

We recently showed that HSPCs can be safely and efficiently mobilized from SCD patients by using Plerixafor<sup>16</sup>. To verify if mobilized SCD HSPCs are permissive to  $\beta$ -AS3 LV transduction, these cells were transduced at an MOI of 36 and of 360. The average  $\beta$ -AS3 VCN per cell increased with the vector dose, reaching 1.22 in erythroblasts, 0.97 in BFU-E and 1.61 in CFU-GM at the highest MOI (n=1 donor; **Figure 5A**). Concomitantly, HbAS3 expression reached 17.97% of total Hb in *in vitro* generated mature RBCs and 16.18% in BFU-E at an MOI of 360 (**Figure 5B**).

We next evaluated  $\beta$ -AS3 gene transfer efficiency in long-term repopulating SCD mobilized HSCs. Mobilized HSPCs from a SCD patient were transduced at an MOI of 100, with a GMP engineering batch of  $\beta$ -AS3 LV, achieving an average VCN of 0.94 and 0.54 copies in *in vitro* generated BFU-E and CFU-GM pools. Mock- and  $\beta$ -AS3-transduced cells were injected into 3 and 4 NSG mice respectively. At 18 weeks after transplantation, we analyzed the engraftment of human hematopoietic cells and average VCN/cell. The

engraftment of mock- and  $\beta$ -AS3-transduced cells was not statistically different in BM, spleen and thymus (**Figure 5C**), with no skewing towards a particular lineage in any of the samples (**Figure S5**). Total human cells derived from the mouse BM were then cultured in a CFC assay. Mock- and  $\beta$ -AS3-transduced samples gave rise to a similar number of BFU-E and CFU-GM with an average VCN of  $0.18 \pm 0.05$  and  $0.16 \pm 0.05$ , respectively (**Figure 5D and 5E**).

Finally, to increase gene transfer efficiency, we transduced healthy donor and SCD mobilized HSPCs using a GMP engineering batch of  $\beta$ -AS3, at an MOI of 100 in the presence of 16,16-dimethyl-prostaglandin E<sub>2</sub> (PGE<sub>2</sub>).<sup>32</sup> PGE<sub>2</sub> treatment led to a 2 to 3.6-fold increase in VCN/cell, leading to  $2.63 \pm 1.07$  and  $1.52 \pm 0.33$  vector copies in BFU-E and CFU-GM derived from SCD Plerixafor-mobilized HSPCs (**Figure 5F**).

## DISCUSSION

In this study, we describe an advanced design of an anti-sickling *HBB* expressing cassette in the context of an LV vector, to expedite high titer vector production and maximize transduction efficiency of human HSPCs while guaranteeing high-level transgene expression for potential use in gene therapy for SCD. We compared two LVs containing an HS2+HS3 or an HS2+HS3+HS4 mini- $\beta$ LCR ( $\beta$ -AS3 and  $\beta$ -AS3 HS4), controlling the expression of a  $\beta^{\text{AS3}}$ -globin transgene containing three anti-sickling amino acid substitutions.<sup>15</sup>

The  $\beta$ -AS3 LV showed a high transduction efficiency of HSPCs from SCD patients, leading to a potentially therapeutic production of  $\beta^{\text{AS3}}$ -globin chains. Importantly, the high transduction efficiency of  $\beta$ -AS3 did not impair erythroid maturation, clonogenic potential and *in vivo* engraftment of transduced HSPCs. A similar LV bearing only HS2 and HS3 sequences was shown to express therapeutic levels of a wild-type *HBB* transgene, thus correcting a murine model of  $\beta$ -thalassemia as well as human  $\beta$ -thalassemic HSPC-derived erythroblasts.<sup>17, 18</sup> In line with these studies, preliminary results of a phase I/II gene therapy clinical trial treating  $\beta$ -thalassemia with this compact LV are very encouraging.<sup>12, 19</sup> However, the impact of the HS4 element in *HBB*-like expressing LVs on transduction efficiency and transgene expression has not previously been reported, particularly in the context of SCD. Importantly, the correction of SCD requires high expression levels of the therapeutic *HBB*-like chain that needs to compete with the endogenous  $\beta^{\text{S}}$ -globin for the incorporation into Hb tetramers, a situation that does not occur in  $\beta$ -thalassemia. Upon inclusion of a 1.1kb HS4 element, LV transduction efficiency was severely affected, with a lower proportion of  $\beta$ -AS3 HS4 vector positive cells and average transgene VCN per transduced cell compared to  $\beta$ -AS3 LV. In addition, in contrast to  $\beta$ -AS3, increasing doses of  $\beta$ -AS3 HS4 did not improve gene transfer efficiency, thereby indicating that the poor performance of the  $\beta$ -AS3-HS4 cannot be

overcome by simply increasing MOI. The superior transduction potential of  $\beta$ -AS3 over  $\beta$ -AS3 HS4 was confirmed *in vivo*, where differences in gene marking were maintained in progenitors derived from long-term repopulating HSCs.

Premature truncation of the  $\beta$ -AS3 HS4 viral transcript occurred, due to a polyadenylation site present within the HS4 element. However, the production of full-length viral genomic RNAs was similar for  $\beta$ -AS3 HS4 and  $\beta$ -AS3 vectors, indicating that the generation of truncated transcripts is not the main determinant of the low  $\beta$ -AS3 HS4 LV titer. The sequence and/or the size of the 1.1-kb HS4 element may impair the production of a high-titer and infective LV by affecting the synthesis or the stability of  $\psi^+$  viral RNAs in the packaging cells. However, the use of a short 304-bp HS4 element restored the  $\psi^+$  viral RNAs levels but did not significantly increase the viral titer and infectivity. Therefore, we hypothesize that the presence of HS4 sequences (e.g., the core HS4 element) might affect other steps of the viral life cycle, such as packaging of the viral RNAs, reverse transcription or integration.

High levels of transgene expression are mandatory for a favorable outcome of gene therapy for SCD patients, where globin chain production from the transgene allows the displacement of the endogenous  $\beta^S$ -globin chain from the hemoglobin tetramers, thus ameliorating the sickling RBC phenotype.<sup>20</sup> Therefore, it was crucial to confirm that the removal of the HS4 element from the mini-LCR does not affect transgene expression, despite the beneficial enhancement in gene transfer efficiency. In transgenic mice harboring the human *HBB* locus, deletion of the 280-bp core element of HS4 leads to a severe *HBB* down-regulation<sup>21</sup>, but deletion of the entire HS4 has a mild effect on *HBB* expression.<sup>22</sup> Interestingly, we show that the HS4 element is dispensable for boosting *HBB* transgene expression in the context of the  $\beta$ -AS3 LV in primary human erythroblasts. Indeed, we detected comparable levels of  $\beta^{\text{AS3}}$ -globin mRNA and HbAS3 tetramers in erythroid cells



derived from samples harboring the same  $\beta$ -AS3 or  $\beta$ -AS3 HS4 average VCN per genome. In another *HBB*-expressing LV, the truncation of the 5' region of the  $\beta$ LCR HS4 element was associated with a higher gene marking in a murine model of  $\beta$ -thalassemia, but lower transgene expression levels, as compared to the LV containing the full HS4.<sup>23</sup> This discrepancy with our study may be ascribed to the potential different activity of HS4 in murine and human erythroid cells. Of note, our vector contains a larger HS2 element (~1.5kb vs 0.8kb<sup>23</sup>) that in combination with only HS3 may be sufficient *per se* to produce high *HBB* transgene expression levels. Importantly, we observed a linear correlation between the vector copies and *HBB* transgene expression for both  $\beta$ -AS3 HS4 and  $\beta$ -AS3 LVs, suggesting that HS4 element is dispensable for integration site position-independent transgene expression.

The remarkable transduction efficiency of SCD HSPCs achieved with  $\beta$ -AS3 combined with the high  $\beta^{\text{AS3}}$ -globin expression levels allowed accumulation of up to 60% therapeutic hemoglobin in terminally differentiated RBCs, levels that were never achieved with the  $\beta$ -AS3 HS4 LV even at high MOI. A concomitant decrease of HbS tetramers was observed, due to the competition of the  $\beta^{\text{AS3}}$ -globin chain for incorporation into Hb tetramers, likely favored by the presence of the A22 amino acidic residue that increases the affinity of the  $\beta^{\text{AS3}}$ -globin for HBA.<sup>15</sup> The sustained anti-sickling  $\beta^{\text{AS3}}$ -globin production (27-47% of HBAS3) together with the beneficial reduction of HbS levels were able to inhibit the formation of hemoglobin polymers and reduce RBC sickling (34-47% of corrected RBCs), proving the efficacy of the  $\beta$ -AS3 LV to reverse the major cellular manifestation of SCD. Of note, in compound heterozygotes of SCD and HPFH, a condition characterized by maintenance of elevated amounts of anti-sickling fetal HBG polypeptides in adult life, HbF levels accounting for as little as 20-30% of the total hemoglobin are associated with the absence of SCD symptoms.<sup>24</sup>

Compared to the BB305 vector, which has given encouraging results in  $\beta$ -thalassaemic patients<sup>25</sup> but not consistently in those with SCD,<sup>13, 14</sup>  $\beta$ -AS3 differs in two key components. First, the mini-*HBB* in  $\beta$ -AS3 contains three anti-sickling amino acid substitutions (G16D, E22A, T87Q) compared to one (T87Q) in BB305,<sup>13</sup> giving  $\beta$ -AS3 a greater anti-sickling activity. Second, the mini- $\beta$ LCR in BB305 consists of the HS2, HS3 and HS4 elements but is only 2.6kb in length whereas the mini- $\beta$ LCR in  $\beta$ -AS3, which although consists of just the HS2 and HS3 sites, spans 2.7kb. Thus the HS core regions in  $\beta$ -AS3 possess considerably larger flanking sequences compared to those in BB305. Given that distance between the core regions of the  $\beta$ LCR HS sites is crucial for effective mutual interaction and chromatin looping leading to  $\beta$ LCR engagement on a downstream promoter for efficient transcriptional activation,<sup>7</sup> the greater compactness of the  $\beta$ LCR HS sites in BB305 could be a disadvantage.

Studies in SCD patients with mixed donor chimerism following allogeneic transplantation indicate that 20% of corrected HSCs are sufficient to reverse the sickle phenotype,<sup>26-28</sup> in all likelihood due to the increased half-life of corrected over unmodified RBCs *in vivo*. In this regard it is noteworthy that we achieved ~20% of transduced long-term repopulating HSCs after transplantation of HSPCs derived from SCD patients either harvested from bone marrow or mobilized using Plerixafor.<sup>16</sup> Plerixafor-mobilized SCD HSPCs represent the only available source of HSCs for a gene therapy approach to SCD, since the administration of the conventional mobilizing agent G-CSF in individuals with SCD leads to severe adverse events<sup>29-31</sup> and the recovery of HSPCs from SCD patients' BM is peculiarly low (M. Cavazzana, unpublished data). Importantly, exposure to PGE<sub>2</sub>, a known molecule that increases gene transfer in long-term repopulating stem cells,<sup>32</sup> enhanced transduction efficiency in SCD Plerixafor-mobilized HSPCs.

In conclusion, in this study we report the functional characterization of a novel and efficient LV expressing an anti-sickling *HBB* transgene in clinically relevant cells from SCD patients as part of a program of work aimed at clinical translation of an effective LV-based gene therapy approach for SCD. Thus, findings of good transduction and expression efficiencies of mobilized HSPCs from SCD patients with the  $\beta$ -AS3 LV bodes well for consistent efficacious future clinical application.

## MATERIALS AND METHODS

### Vector construction

The expression cassette consisting of DNase I hypersensitive sites HS2 (genomic coordinates[hg38]: chr11:5280255-5281665) and HS3 (genomic coordinates[hg38]: chr11:5284251-5285452) of the locus control region ( $\beta$ LCR)<sup>33</sup> and *HBB* mini-gene extending from -265bp upstream of the transcriptional start site to +300bp downstream of the poly(A)-addition site (genomic coordinates[hg38]: chr11:5225174-5227336) with a short version of intron 2 (genomic coordinates[hg38]: chr11:5203703-5204295),<sup>17</sup> was cloned into a pCCL lentiviral vector backbone<sup>34</sup> to generate the pCCL. $\beta$ -globin plasmid. The mutations determining three anti-sickling amino acid substitutions (G16D, E22A and T87Q)<sup>15</sup> were introduced in the pCCL. $\beta$ -globin plasmid by *in vitro* site-directed mutagenesis to obtain the pCCL. $\beta$ -AS3 plasmid. The addition of the  $\beta$ LCR HS4 element (genomic coordinates[hg38]: chr11:5287846-5288936)<sup>33</sup> or of the short HS4 fragment (genomic coordinates[hg38]: chr11:5288094-5288397) containing the core HS4 element, to generate the pCCL. $\beta$ -AS3 HS4 and the pCCL. $\beta$ -AS3 HS4 core plasmids, was achieved by replacing the HS2/HS3 sequence of pCCL. $\beta$ -AS3 with a commercially synthesized (GeneWiz, South Plainfield, NJ, USA) fragment containing a combination of  $\beta$ LCR HS2/HS3/HS4 sites as previously described.<sup>35</sup>

### Lentiviral vector production and titration

Third-generation lentiviral vectors were produced by calcium phosphate transient transfection of HEK293T cells of the transfer vector (pCCL. $\beta$ -AS3 or pCCL. $\beta$ -AS3 HS4), the packaging plasmid pKlg/p.RRE, the Rev-encoding plasmid pK.REV, and the vesicular stomatitis virus glycoprotein G (VSV-G) envelope-encoding plasmid pK.G, as previously described.<sup>36</sup> The physical titer of vector preparations was measured using the HIV-1 Gag p24 antigen

immunocapture assay kit (PerkinElmer, Waltham, MA, USA) and expressed as p24ng/mL. The viral infectious titer was calculated by transducing HCT116, K562 and HEL cells. HCT116 cells were transduced with serial vector dilutions, as previously described.<sup>37</sup> K562 and HEL cells were transduced overnight with serial dilutions of the virus in DMEM medium supplemented of 10% fetal bovine serum (Gibco, Carlsbad, CA, USA), penicillin/streptomycin (Gibco, Carlsbad, CA, USA), glutamine (Gibco, Carlsbad, CA, USA) and polybrene (8 µg/ml, Sigma-Aldrich, St. Louis, MI, USA). After transduction, cells were washed and maintained in complete DMEM medium for one week before determining vector copy number (VCN) per genome. VCN was used to calculate the viral infectious titer, expressed as transducing units per ml (TU/ml). Viral infectivity was calculated as ratio between infectious and physical titers (TU/ng p24).

### **Viral transcript quantification**

Total RNA was extracted from HEK293T cells transfected as described above (“Viral vector preparation”), using the RNeasy kit (Qiagen, Venlo, Netherlands), which included an in-column DNase-I treatment step. An additional DNase treatment was performed after RNA purification using the TURBO DNA-free Kit (Ambion, Waltham, MA, USA). Then, RNA was reverse-transcribed by extension of random hexamers using the SuperScript III First-Strand Synthesis kit (Invitrogen, Carlsbad, CA, USA). As negative controls, RNA samples were treated without reverse transcriptase (RT). We performed duplex TaqMan RT-qPCR to quantify total  $\psi^+$  and full-length viral transcripts. GAPDH was used as an internal reference standard for RNA normalization.

Primers and probes used for TaqMan RT-qPCR are listed below:

HIV1-RNAfullLenght 3 (ΔU3) FOR 5’-CAGCTGTAGATCTTAGCCACTTT-3’

HIV1-RNAfullLenght (ΔU3) REV 5’-AGCAGATCTTGTCTTCGTTGG-3’

HIV1-RNAfullLenght (ΔU3) PROBE-fam AS 5’-AGTGAATTAGCCCTTCCAGTCCC-3’

HIV1-PSI FOR 5'-CAGGACTCGGCTTGCTGAAG-3'

HIV1-PSI REV 5'-TCCCCCGCTTAATACTGACG-3',

HIV1-PSI PROBE-fam 5'-CGCACGGCAAGAGGCGAGG-3'

GAPDH FOR 5'-CTTCATTGACCTCAACTACATGGTTT-3'

GAPDH REV 5'-TGGGATTTCATTGATGACAAG-3'

GAPDH PROBE-vic 5'-CAAATTCCATGGCACCGTCAAGGC-3'

### **Identification of truncated viral transcripts**

Total RNA was extracted from packaging HEK293T cells following transfection for vector packaging and reverse-transcribed by using the 3' RACE Kit (Invitrogen, Carlsbad, CA, USA), in accordance with the manufacturer's instructions. To identify any transcripts with pre-mature polyadenylation within the HS4 region, we used a forward primer annealing to the HS3 region (HS3 primer 5'-CTCTTACTCATCCCATCACGTATGC-3') and the UAP primer provided in the kit as reverse primer (5'-CUACUACUACUAGGCCACGCGTCGACTAGTAC-3'). The 3' RACE PCR product was loaded on a 1% agarose gel and the amplicons were visualized by GelRed (Biotium, Fremont, CA, USA) staining. After electrophoresis, the amplicons were extracted from the gel, cloned using the StrataClone PCR Cloning Kit (Agilent, Santa Clara, CA, USA) and analyzed by Sanger sequencing.

### **HSPC purification and transduction**

We obtained human adult CD34<sup>+</sup> HSPCs mobilized with G-CSF from healthy donors. Human adult SCD HSPCs were either harvested from bone marrow or mobilized using Plerixaflor (NCT 02212535 clinical trial, Necker Hospital, Paris, France). Written informed consent was obtained from all subjects. All experiments were performed in accordance with the Declaration of Helsinki. The study was approved by the regional investigational review

board (reference: DC 2014-2272, CPP Ile-de-France II “Hôpital Necker-Enfants malades”). HSPCs were purified by immunomagnetic selection with AutoMACS (Miltenyi Biotec, Bergisch Gladbach, Germany) after immunostaining with CD34 MicroBead Kit (Miltenyi Biotec, Bergisch Gladbach, Germany).

CD34<sup>+</sup> cells (10<sup>6</sup> cells/ml) were pre-activated for 24 h in X-VIVO 20 supplemented with penicillin/streptomycin (Gibco, Carlsbad, CA, USA) and the following recombinant human cytokines (obtained from either CellGenix GmbH, Freiburg, Germany or Peprotech, London, UK): 300 ng/ml SCF, 300 ng/ml Flt-3L, 100 ng/ml TPO and 20 ng/ml IL3. After pre-activation, cells (10<sup>6</sup> cells/ml) were transduced for 24 hours in plates coated with RetroNectin (10 µg/cm<sup>2</sup>, Takara Bio, Kusatsu, Japan), in the pre-activation medium supplemented with protamine sulfate (4 µg/ml, Sigma-Aldrich, St. Louis, MI, USA or APP Pharmaceuticals, Schaumburg, IL, USA). Transductions using 16,16-dimethyl-prostaglandin E<sub>2</sub> (PGE<sub>2</sub>; Cayman Chemical) efficacy were performed using conditions previously described.<sup>13, 32</sup> Multiplicity of infection (MOI) was calculated using the viral infectious titer determined in HCT116 cells.

### ***In vitro* erythroid differentiation**

A 3-step protocol<sup>38</sup> was adapted to generate mature RBCs from mock- and LV-transduced CD34<sup>+</sup> cells. From days 0 to 6, cells were grown in a basal erythroid medium supplemented with the following recombinant human cytokines: 100 ng/mL SCF (Peprotech, London, UK), 5 ng/mL IL3 (Peprotech, London, UK), and 3 IU/mL of EPO Eprex (Janssen-Cilag, Issy-Les-Moulineaux, France), and hydrocortisone (Sigma, St. Louis, MI, USA) at 10<sup>-6</sup> M. From days 6 to 9, cells were cultured onto a layer of murine stromal MS-5 cells in basal erythroid medium supplemented only with 3 IU/mL EPO Eprex. Finally, from days 9 to 20, cells were continued to be cultured on a layer of MS-5 cells in basal erythroid medium but without

cytokines. Erythroid differentiation was monitored by May Grunwald-Giemsa staining, flow cytometry analysis of the erythroid surface markers CD36 (CD36-V450, BD Horizon, Franklin Lakes, NJ, USA), CD71 (CD71-FITC, BD Pharmingen, Franklin Lakes, NJ, USA) and GYPA (CD235a-PECY7, BD Pharmingen, Franklin Lakes, NJ, USA). We used the nuclear dye DRAQ5 (eBioscience, San Diego, CA, USA) to evaluate the proportion of enucleated RBCs. Flow cytometry analyses were performed using the Gallios analyzer and Kaluza software (Beckman-Coulter, Brea, CA, USA).

### **CFC Assay**

The number of hematopoietic progenitors was evaluated by a clonal Colony Forming Cell (CFC) assay, where HSPCs were plated at  $1 \times 10^3$  cells/ml in methylcellulose-containing medium (GFH4435, Stem Cell Technologies, Vancouver, BC, USA) under conditions supporting both erythroid and granulo-monocytic differentiation. Numbers of BFU-E and CFU-GM colonies were scored after 14 days. BFU-E were randomly picked and collected as bulk populations (containing at least 25 colonies) or individual BFU-E to evaluate the efficiency of transduction and hemoglobin expression.

### **Vector copy number analysis**

At day 13 of erythroid differentiation, or 14 days after plating HSPCs in the methylcellulose medium, DNA was extracted from transduced cells using the ReliaPrep Blood gDNA Miniprep System (Promega, Madison, WI, USA) or the DNA Extract All Reagents Kit (ThermoFisher Scientific, Waltham, MA, USA). VCN per diploid genome was determined by duplex Taqman quantitative PCR (qPCR) (Applied Biosystems, Foster City, CA, USA), as previously described.<sup>37</sup> We used primers and probes specific for: (i) the viral  $\psi$  (PSI) packaging signal (HIV1-PSI FOR 5'-CAGGACTCGGCTTGCTGAAG-3', HIV1-PSI REV



5'-TCCCCCGCTTAATACTGACG-3', HIV1-PSI PROBE 5'-  
 CGCACGGCAAGAGGCGAGG-3') and (ii) the human albumin gene (*ALB*), as an internal  
 reference standard (ALB FOR 5'-GCTGTCATCTCTTGTGGGCTGT-3', ALB REV 5'-  
 ACTCATGGGAGCTGCTGGTTC-3', ALB PROBE 5'-  
 CCTGTCATGCCCACACAAATCTCTCC-3'). Standard curves were obtained by serial  
 dilutions of a plasmid containing one copy of  $\psi$  and *ALB* sequences. The number of PSI and  
*ALB* copies in test samples were extrapolated from the standard curves.

### RT-qPCR analysis of globin transcripts

At day 13 of erythroid differentiation, or 14 days after plating HSPCs in the methylcellulose medium, RNA was extracted using RNeasy micro kit (Qiagen, Venlo, Netherlands). Reverse transcription of mRNA employed the SuperScript First-Strand Synthesis System for RT-PCR (Invitrogen, Carlsbad, CA, USA) with oligo(dT) primers. RT-qPCR was performed using SYBR green (Applied Biosystems, Foster City, CA, USA) as a detection system with the following primers:

HBBAS3 F: 5'-AAGGGCACCTTTGCCCAG-3'

HBBAS3 R: 5'-GCCACCACTTTCTGATAGGCAG-3'

HBB F: 5'-AAGGGCACCTTTGCCACA-3'

HBB R: 5'-GCCACCACTTTCTGATAGGCAG-3'

### Cation-exchange HPLC analysis of hemoglobin tetramers

Cation-exchange HPLC analysis was performed using a NexeraX2 SIL-30AC chromatograph (Shimadzu, Kyoto, Japan) and the LC Solution software. Hemoglobin tetramers from mature RBCs or BFU-E were separated by HPLC using a 2 cation-exchange

column (PolyCAT A, PolyLC, Columbia, MD, USA). Samples were eluted with a gradient mixture of solution A (20mM bis Tris, 2mM KCN, pH=6.5) and solution B (20mM bis Tris, 2mM KCN, 250mM NaCl, pH=6.8). The absorbance was measured at 415 nm.

### **Sickling assay**

RBCs at day-20 of erythroid differentiation, derived from transduced and mock transduced SCD HSPCs, were exposed to an oxygen-deprived atmosphere (0% O<sub>2</sub>) for at least 35 minutes before image capture, using the AxioObserver Z1 microscope (Zeiss, Oberkochen, Germany) and a 20X objective. Images were processed with ImageJ to determine the percentage of sickled RBCs per field of acquisition in the total RBC population.

### **NSG mouse transplantation**

Non-obese diabetic severe combined immunodeficiency gamma (NSG) mice (NOD.CgPrkdcscid Il2rgtm1Wj/SzJ, Charles River Laboratories, St Germain sur l'Arbresle, France) were housed in a specific pathogen-free facility. Mice at 6 to 8-weeks of age were conditioned with busulfan (Sigma, St Louis, MO, US) injected intraperitoneally (25mg/kg body weight/day) 24h, 48h and 72h before transplantation. Mock- or LV-transduced CD34<sup>+</sup> cells (500,000 cells/mouse for SCD BM, HD mPB and HD CB HSPCs and 10<sup>6</sup> cells/mouse for SCD mobilized HSPCs) were transplanted into NSG mice via retro-orbital sinus injection. Neomycin and acid water were added in the water bottle. At 10 to 19 weeks post-transplantation, NSG recipients were sacrificed. Cells were harvested from femur BM, thymus and spleen, stained with antibodies against murine or human surface markers (murine CD45, BD Biosciences, Franklin Lakes, NJ, USA; human CD45, Miltenyi Biotec, Bergisch Gladbach, Germany; human CD3, Miltenyi Biotec, Bergisch Gladbach, Germany; human CD14, BD Biosciences, Franklin Lakes, NJ, USA; human CD15, Beckman Coulter, Brea,

CA, USA; human CD19, Sony Biotechnologies, San Jose, CA, USA; human CD36, BD Biosciences, Franklin Lakes, NJ, USA), and analyzed by flow cytometry using a Gallios analyzer and the Kaluza software (Beckman-Coulter, Brea, CA, USA). 100,000 BM cells were subjected to the CFC Assay, and BFU-E and CFU-GM pools were analyzed for VCN. All experiments and procedures were performed in compliance with the French Ministry of Agriculture's regulations on animal experiments and were approved by the regional Animal Care and Use Committee (APAFIS#2101-2015090411495178 v4).

### **Statistical analyses**

Unpaired t tests were performed to compare vector titer and infectivity, viral genomic RNA levels, VCN/cell and the engraftment rate between 2 groups. We used one-way ANOVA test when comparing the engraftment rate between >2 groups. We performed Chi-squared test (2-sample test for equality of proportions with continuity correction) to compare the frequency of transduced CFC. Linear regression analyses were performed to assess the correlation between VCN/cell and transgene expression. All statistical analyses were performed using Prism4 software (GraphPad, La Jolla, CA, USA). The threshold for statistical significance was set to  $P < 0.05$ .

## AUTHOR CONTRIBUTIONS

L.W. and V.P. designed and conducted experiments, and wrote the paper, E.M., C.A., S.M. V.M., and S.E.L., designed and conducted experiments, C.B., H.S. and T.F. conducted experiments, W.E.N. contributed to the design of the experimental strategy. FM, M.C. and I.A.S. conceived the study. MNA assisted with the drafting of the manuscript. AM conceived the study, designed experiments and wrote the paper.

## ACKNOWLEDGEMENTS

This work was supported by grants from AFM-Telethon (17224), the European Research Council (ERC-2010-AdG, GT-SKIN; ERC-2015-AdG, GENEFORCURE), *Agence nationale de la recherche* (ANR-16-CE18-0004 and ANR-10-IAHU-01 “Investissements d’avenir” program) and the EU Marie Curie-COFUND (PRESTIGE\_2015\_2\_0015) program and by a collaboration with BioMarin Pharmaceutical Inc.

## DISCLOSURE/CONFLICT OF INTEREST

The Authors have no conflict of interest.

## REFERENCES

1. Piel, FB, Patil, AP, Howes, RE, Nyangiri, OA, Gething, PW, Dewi, M, *et al.* (2013). Global epidemiology of sickle haemoglobin in neonates: a contemporary geostatistical model-based map and population estimates. *Lancet* **381**: 142-151.
2. Steinberg, MH, Barton, F, Castro, O, Pegelow, CH, Ballas, SK, Kutlar, A, *et al.* (2003). Effect of hydroxyurea on mortality and morbidity in adult sickle cell anemia: risks and benefits up to 9 years of treatment. *JAMA* **289**: 1645-1651.
3. Chandrakasan, S, and Malik, P (2014). Gene therapy for hemoglobinopathies: the state of the field and the future. *Hematol Oncol Clin North Am* **28**: 199-216.
4. Pawliuk, R, Westerman, KA, Fabry, ME, Payen, E, Tighe, R, Bouhassira, EE, *et al.* (2001). Correction of sickle cell disease in transgenic mouse models by gene therapy. *Science (New York, NY)* **294**: 2368-2371.
5. Perumbeti, A, Higashimoto, T, Urbinati, F, Franco, R, Meiselman, HJ, Witte, D, *et al.* (2009). A novel human gamma-globin gene vector for genetic correction of sickle cell anemia in a humanized sickle mouse model: critical determinants for successful correction. *Blood* **114**: 1174-1185.
6. Romero, Z, Urbinati, F, Geiger, S, Cooper, AR, Wherley, J, Kaufman, ML, *et al.* (2013). beta-globin gene transfer to human bone marrow for sickle cell disease. *J Clin Invest.*
7. Kim, A, and Dean, A (2012). Chromatin loop formation in the beta-globin locus and its role in globin gene transcription. *Mol Cells* **34**: 1-5.
8. May, C, Rivella, S, Callegari, J, Heller, G, Gaensler, KM, Luzzatto, L, *et al.* (2000). Therapeutic haemoglobin synthesis in beta-thalassaemic mice expressing lentivirus-encoded human beta-globin. *Nature* **406**: 82-86.

9. Persons, DA, Hargrove, PW, Allay, ER, Hanawa, H, and Nienhuis, AW (2003). The degree of phenotypic correction of murine beta -thalassemia intermedia following lentiviral-mediated transfer of a human gamma-globin gene is influenced by chromosomal position effects and vector copy number. *Blood* **101**: 2175-2183.
10. Molete, JM, Petrykowska, H, Bouhassira, EE, Feng, YQ, Miller, W, and Hardison, RC (2001). Sequences flanking hypersensitive sites of the beta-globin locus control region are required for synergistic enhancement. *Molecular and cellular biology* **21**: 2969-2980.
11. Cavazzana, M, Antoniani, C, and Miccio, A (2017). Gene Therapy for beta-Hemoglobinopathies. *Mol Ther* **25**: 1142-1154.
12. Ferrari, G, Cavazzana, M, and Mavilio, F (2017). Gene Therapy Approaches to Hemoglobinopathies. *Hematol Oncol Clin North Am* **31**: 835-852.
13. Ribeil, JA, Hacein-Bey-Abina, S, Payen, E, Magnani, A, Semeraro, M, Magrin, E, *et al.* (2017). Gene Therapy in a Patient with Sickle Cell Disease. *N Engl J Med* **376**: 848-855.
14. Kanter, J, Walters, MC, Hsieh, MM, Krishnamurti, L, Kwiatkowski, J, Kamble, RT, *et al.* (2016). Interim Results from a Phase 1/2 Clinical Study of Lentiglobin Gene Therapy for Severe Sickle Cell Disease. *ASH 58th Annual Meeting*.
15. Levasseur, DN, Ryan, TM, Reilly, MP, McCune, SL, Asakura, T, and Townes, TM (2004). A recombinant human hemoglobin with anti-sickling properties greater than fetal hemoglobin. *J Biol Chem* **279**: 27518-27524.
16. Lagresle-Peyrou, C, Lefrere, F, Magrin, E, Ribeil, JA, Romano, O, Weber, L, *et al.* (2018). Plerixafor enables the safe, rapid, efficient mobilization of haematopoietic stem cells in sickle cell disease patients after exchange transfusion. *Haematologica*.

17. Miccio, A, Cesari, R, Lotti, F, Rossi, C, Sanvito, F, Ponzoni, M, *et al.* (2008). In vivo selection of genetically modified erythroblastic progenitors leads to long-term correction of beta-thalassemia. *Proceedings of the National Academy of Sciences of the United States of America* **105**: 10547-10552.
18. Roselli, EA, Mezzadra, R, Frittoli, MC, Maruggi, G, Biral, E, Mavilio, F, *et al.* (2010). Correction of beta-thalassemia major by gene transfer in haematopoietic progenitors of pediatric patients. *EMBO Mol Med* **2**: 315-328.
19. Ferrari, G (2016). Gene Therapy: The Challenge of Correcting Hemoglobinopathies. *ASH 58th Annual Meeting*.
20. Ribeil, JA, Hacein-Bey-Abina, S, Payen, E, Magnani, A, Semeraro, M, Magrin, E, *et al.* (2017). Gene Therapy in a Patient with Sickle Cell Disease. *New England Journal of Medicine* **in press**.
21. Navas, PA, Peterson, KR, Li, Q, McArthur, M, and Stamatoyannopoulos, G (2001). The 5'HS4 core element of the human beta-globin locus control region is required for high-level globin gene expression in definitive but not in primitive erythropoiesis. *J Mol Biol* **312**: 17-26.
22. Fedosyuk, H, and Peterson, KR (2007). Deletion of the human beta-globin LCR 5'HS4 or 5'HS1 differentially affects beta-like globin gene expression in beta-YAC transgenic mice. *Blood Cells Mol Dis* **39**: 44-55.
23. Lisowski, L, and Sadelain, M (2007). Locus control region elements HS1 and HS4 enhance the therapeutic efficacy of globin gene transfer in beta-thalassemic mice. *Blood* **110**: 4175-4178.
24. Ngo, DA, Aygun, B, Akinsheye, I, Hankins, JS, Bhan, I, Luo, HY, *et al.* (2012). Fetal haemoglobin levels and haematological characteristics of compound heterozygotes

- for haemoglobin S and deletional hereditary persistence of fetal haemoglobin. *Br J Haematol* **156**: 259-264.
25. Thompson, AA, Walters, MC, Kwiatkowski, J, Rasko, JEJ, Ribeil, JA, Hongeng, S, *et al.* (2018). Gene Therapy in Patients with Transfusion-Dependent beta-Thalassemia. *N Engl J Med* **378**: 1479-1493.
  26. Altrock, PM, Brendel, C, Renella, R, Orkin, SH, Williams, DA, and Michor, F (2016). Mathematical modeling of erythrocyte chimerism informs genetic intervention strategies for sickle cell disease. *Am J Hematol* **91**: 931-937.
  27. Walters, MC, Patience, M, Leisenring, W, Rogers, ZR, Aquino, VM, Buchanan, GR, *et al.* (2001). Stable mixed hematopoietic chimerism after bone marrow transplantation for sickle cell anemia. *Biol Blood Marrow Transplant* **7**: 665-673.
  28. Abraham, A, Hsieh, M, Eapen, M, Fitzhugh, C, Carreras, J, Keesler, D, *et al.* (2017). Relationship between Mixed Donor-Recipient Chimerism and Disease Recurrence after Hematopoietic Cell Transplantation for Sickle Cell Disease. *Biol Blood Marrow Transplant* **23**: 2178-2183.
  29. Abboud, M, Laver, J, and Blau, CA (1998). Granulocytosis causing sickle-cell crisis. *Lancet* **351**: 959.
  30. Adler, BK, Salzman, DE, Carabasi, MH, Vaughan, WP, Reddy, VV, and Prchal, JT (2001). Fatal sickle cell crisis after granulocyte colony-stimulating factor administration. *Blood* **97**: 3313-3314.
  31. Grigg, AP (2001). Granulocyte colony-stimulating factor-induced sickle cell crisis and multiorgan dysfunction in a patient with compound heterozygous sickle cell/beta+ thalassemia. *Blood* **97**: 3998-3999.
  32. Zonari, E, Desantis, G, Petrillo, C, Boccalatte, FE, Lidonnici, MR, Kajaste-Rudnitski, A, *et al.* (2017). Efficient Ex Vivo Engineering and Expansion of Highly Purified



- Human Hematopoietic Stem and Progenitor Cell Populations for Gene Therapy. *Stem Cell Reports* **8**: 977-990.
33. Hardison, R, Slightom, JL, Gumucio, DL, Goodman, M, Stojanovic, N, and Miller, W (1997). Locus control regions of mammalian beta-globin gene clusters: combining phylogenetic analyses and experimental results to gain functional insights. *Gene* **205**: 73-94.
34. Follenzi, A, Sabatino, G, Lombardo, A, Boccaccio, C, and Naldini, L (2002). Efficient gene delivery and targeted expression to hepatocytes in vivo by improved lentiviral vectors. *Hum Gene Ther* **13**: 243-260.
35. Montiel-Equihua, CA, Zhang, L, Knight, S, Saadeh, H, Scholz, S, Carmo, M, *et al.* (2012). The beta-globin locus control region in combination with the EF1alpha short promoter allows enhanced lentiviral vector-mediated erythroid gene expression with conserved multilineage activity. *Mol Ther* **20**: 1400-1409.
36. Cantore, A, Ranzani, M, Bartholomae, CC, Volpin, M, Valle, PD, Sanvito, F, *et al.* (2015). Liver-directed lentiviral gene therapy in a dog model of hemophilia B. *Sci Transl Med* **7**: 277ra228.
37. Lattanzi, A, Duguez, S, Moiani, A, Izmiryan, A, Barbon, E, Martin, S, *et al.* (2017). Correction of the Exon 2 Duplication in DMD Myoblasts by a Single CRISPR/Cas9 System. *Mol Ther Nucleic Acids* **7**: 11-19.
38. Giarratana, MC, Kobari, L, Lapillonne, H, Chalmers, D, Kiger, L, Cynober, T, *et al.* (2005). Ex vivo generation of fully mature human red blood cells from hematopoietic stem cells. *Nature biotechnology* **23**: 69-74.

## FIGURE LEGENDS

**Figure 1. Characterization of  $\beta$ -AS3 HBB expressing LVs.** (A) Schematic representation of  $\beta$ -AS3 HS4 and  $\beta$ -AS3 lentiviral vectors.  $\Delta$ , deleted HIV-1 U3 region; SD and SA, HIV Splicing Donor and Acceptor sites;  $\psi$ , HIV-1 packaging signal; RRE, HIV-1 Rev Responsive Element; Ex, exons of the human *HBB*;  $\beta$ p, promoter of *HBB*; HS2, 3 and 4: DNase I hypersensitive site 2, 3 and 4 of human *HBB* LCR; red arrows indicate the mutations introduced in exon 1 (generating amino acid substitutions G16D and E22A) and exon 2 (generating amino acid substitution T87Q). (B) The histograms show the physical and infectious titers and infectivity of  $\beta$ -AS3 HS4 and  $\beta$ -AS3 LVs. Infectious titer and infectivity were measured in HTC116 (5 different preparations for each vector) and K562 and HEL erythroid cell lines (2 viral preparations per vector). (C) Vector copy number (VCN) in G-CSF-mobilized CD34<sup>+</sup> cells from healthy donors (HD). HSPCs were transduced with increasing amounts of three and two preparations of  $\beta$ -AS3 and  $\beta$ -AS3 HS4 LVs, respectively. Cells were grown in liquid culture and after one week VCN was determined. A linear correlation between  $\beta$ -AS3 vector dose and VCN is obtained, whereas a modest increase in VCN was achieved by transducing HSPCs with higher amounts of  $\beta$ -AS3 HS4 vector preparations. (D) Relative quantification of the  $\psi$ <sup>+</sup> viral genomic RNA produced by HEK293T packaging cells (n=3) by RT-qPCR. The  $\beta$ -AS3 sample was used as a calibrator. Data were plotted as mean $\pm$ SD (unpaired t-test). \*,  $P\leq 0.05$ , \*\*,  $P\leq 0.01$ , \*\*\*\*,  $P\leq 0.0001$ , ns, not significant.

**Figure 2. Gene transfer efficiency in SCD patient-derived BM HSPCs transduced with  $\beta$ -AS3 HS4 and  $\beta$ -AS3 LVs.** (A) Percentages of CD34<sup>+</sup> HSPCs that gave rise to BFU-E and CFU-GM in CFC assay. Values shown are mean $\pm$ SEM of 3 to 5 independent experiments. (B) Average VCN/cell in bulk populations of erythroblasts grown in liquid culture, and pools

of BFU-E and CFU-GM derived from  $\beta$ -AS3 HS4- and  $\beta$ -AS3-transduced SCD BM HSPCs. Values shown are mean $\pm$ SEM of 2 to 6 independent experiments (n=2 donors). \*,  $P\leq 0.05$  (unpaired t-test). (C) Percentage of vector<sup>+</sup> BFU-E and CFU-GM derived from SCD BM HSPCs transduced with  $\beta$ -AS3 HS4. Values shown are mean $\pm$ SEM of 3 to 6 independent experiments (n=2 donors). \*\*\*,  $P\leq 0.001$ , \*\*\*\*,  $P\leq 0.0001$  (chi squared test) (D) Clonal analysis of VCN in BFU-E and CFU-GM colonies derived from SCD BM HSPCs transduced with  $\beta$ -AS3 HS4 or  $\beta$ -AS3. Values shown are mean $\pm$ SEM of 3 to 6 independent experiments (n=2 donors). A higher proportion of colonies harboring >3 VCN was observed for  $\beta$ -AS3 LV at MOIs of 36 and 360 ( $P\leq 0.001$ ; chi squared test).

**Figure 3.  $\beta$ -AS3 HS4 and  $\beta$ -AS3 transduction efficiencies in long-term repopulating SCD HSCs.** (A) Engraftment of human cells in NSG mice transplanted with mock and LV-transduced SCD BM CD34<sup>+</sup> cells (MOI=360, n=5 mice for each group), and HD mPB (n=3) and HD CB (n=2) HSPCs, 15 weeks after transplantation. Engraftment is represented as percentage of human CD45<sup>+</sup> cells in the total murine and human CD45<sup>+</sup> cell population, in BM, spleen and thymus. Values shown are mean $\pm$ SEM. ns, not significant (One-way ANOVA test). (B) Human hematopoietic progenitor content in BM mononuclear cells (MNC) derived from mice transplanted with either mock- or  $\beta$ -AS3 HS4- and  $\beta$ -AS3-transduced SCD BM HSPCs. We plotted the percentage of BM MNC giving rise to BFU-E and CFU-GM. Values shown are mean $\pm$ SEM of 4 samples per condition. (C) VCN/cell in pools of BFU-E and CFU-GM derived from total BM MNC, obtained from mice injected with SCD BM HSPCs transduced with  $\beta$ -AS3 HS4 (n=2 and n=3 for BFU-E and CFU-GM, respectively) and  $\beta$ -AS3 (n=3 and n=4 for BFU-E and CFU-GM, respectively) LVs at an MOI of 360. Values shown are mean $\pm$ SEM. \*,  $P\leq 0.05$  (unpaired t-test).

**Figure 4. Transgene expression in erythroid cells derived from  $\beta$ -AS3 HS4- and  $\beta$ -AS3-transduced SCD BM HSPCs and phenotypic correction of SCD RBCs by  $\beta$ -AS3.** (A) *HBBAS3* mRNA expression was measured by RT-qPCR in erythroblasts at day-13 post induction of erythroid differentiation, normalized using the endogenous  $\beta^S$ -globin gene (*HBBS*), and correlated with VCN/cell. The slopes of the linear regression lines for samples derived from  $\beta$ -AS3 HS4- and  $\beta$ -AS3-transduced HSPCs were not significantly different ( $P=0.2922$ ). Equations that define the best fit lines were:  $y = 0.13x - 0.011$  ( $R^2=1.0$  and  $P<0.0001$ ) for  $\beta$ -AS3 HS4 samples and  $y = 0.10x - 0.00059$  ( $R^2=0.99$  and  $P<0.0001$ ) for  $\beta$ -AS3 samples. 5  $\beta$ -AS3 HS4- and 10  $\beta$ -AS3-transduced samples were analyzed ( $n=2$  donors). (B) HbAS3 was quantified by cation-exchange HPLC in RBCs at day 20 of erythroid differentiation. The percentage of HbAS3 in the total adult Hb (HbAS3+HbS) was correlated with the average VCN/cell. Upper panel: The slopes of the linear regression lines for RBC samples derived from  $\beta$ -AS3 HS4- and  $\beta$ -AS3-transduced HSPCs were not significantly different ( $P=0.1446$ ) (line-of-best-fit equation:  $y = 20.79x - 0.49$ ,  $R^2=0.9905$  and  $P=0.0004$  for  $\beta$ -AS3 HS4 samples and  $y = 8.08x + 6.10$ ,  $R^2=0.8776$  and  $P<0.0001$  for  $\beta$ -AS3 samples). 5  $\beta$ -AS3 HS4- and 11  $\beta$ -AS3-transduced samples were analyzed ( $n=2$  donors). Bottom right panel: plot of HbAS3 expression in RBCs derived from  $\beta$ -AS3 HS4- and  $\beta$ -AS3-transduced samples harboring a similar VCN/cell. Bottom left panel: HbAS3 expression per VCN/cell. Data were plotted as mean $\pm$ SEM (unpaired t-test). ns, not significant. (C) HPLC chromatograms of RBC lysates obtained after 20 days of erythroid differentiation of mock- and LV-transduced SCD BM HSPCs. (D-F) *In vitro* sickling assay measuring the proportion of sickled RBC under hypoxic conditions (0%  $O_2$ ). Representative photomicrographs of RBCs derived from mock- and  $\beta$ -AS3-transduced samples at 0% of  $O_2$  are shown (D; SCD donor 1). Scale bars, 20  $\mu$ m. The percentage of corrected RBCs was correlated to the VCN/cell (E) or to HbAS3 expression (F) for 2 SCD donors. The proportion of corrected

cells was calculated as the percentage of non-sickled cells in the transduced samples, minus the percentage of non-sickled cells in the corresponding mock-transduced sample. Values are mean $\pm$ SEM of 3 and 4 microscopic fields for donor 1 and donor 2, respectively. For donor 2, a higher VCN and transgene expression was necessary to achieve a frequency of corrected RBCs comparable to the value observed for donor 1. This difference may be due to the coinheritance of different genetic disease modifiers along with the SCD mutation.

**Figure 5. *In vitro* and *in vivo* gene transfer efficiency in cells derived from SCD Plerixafor-mobilized  $\beta$ -AS3-transduced HSPCs.** (A) VCN/cell in bulk populations of erythroblasts, and in pools of BFU-E and CFU-GM derived from  $\beta$ -AS3-transduced SCD Plerixafor mobilized HSPCs. Transductions were performed using MOI of 36 and 360. (B) HbAS3 expression was quantified by cation-exchange HPLC in BFU-E and RBCs. Average VCN/cell is indicated. (C) Engraftment of human CD45<sup>+</sup> cells derived from SCD mobilized samples in BM, spleen and thymus of NSG mice, 18 weeks after transplantation. Plerixafor-mobilized SCD HSPCs were transduced with  $\beta$ -AS3 LV at an MOI of 100. Values shown are mean $\pm$ SEM (n=2 and n=4 mice for mock- and  $\beta$ -AS3-transduced samples, respectively). ns, not significant (Unpaired t-test). (D) Human hematopoietic progenitor content in BM MNC obtained from mice transplanted with mock- or  $\beta$ -AS3-transduced SCD Plerixafor-mobilized HSPCs. We plotted the percentage of BM MNC giving rise to BFU-E and CFU-GM. Values shown are mean $\pm$ SEM of 2 and 4 samples obtained from mice receiving mock- and  $\beta$ -AS3-transduced cells, respectively. (E) Average VCN/cell in pools of BFU-E and CFU-GM derived from the BM of mice injected with SCD Plerixafor-mobilized HSPCs transduced with  $\beta$ -AS3 (n=4). Values shown are mean $\pm$ SEM. (F) Average VCN/cell in pools of BFU-E and CFU-GM obtained from mobilized HSPCs of a healthy donor (HD mPB) and a SCD

patient (SCD mPB), transduced with  $\beta$ -AS3  $\pm$  PGE<sub>2</sub>. Values shown are mean $\pm$ SEM of technical replicates.

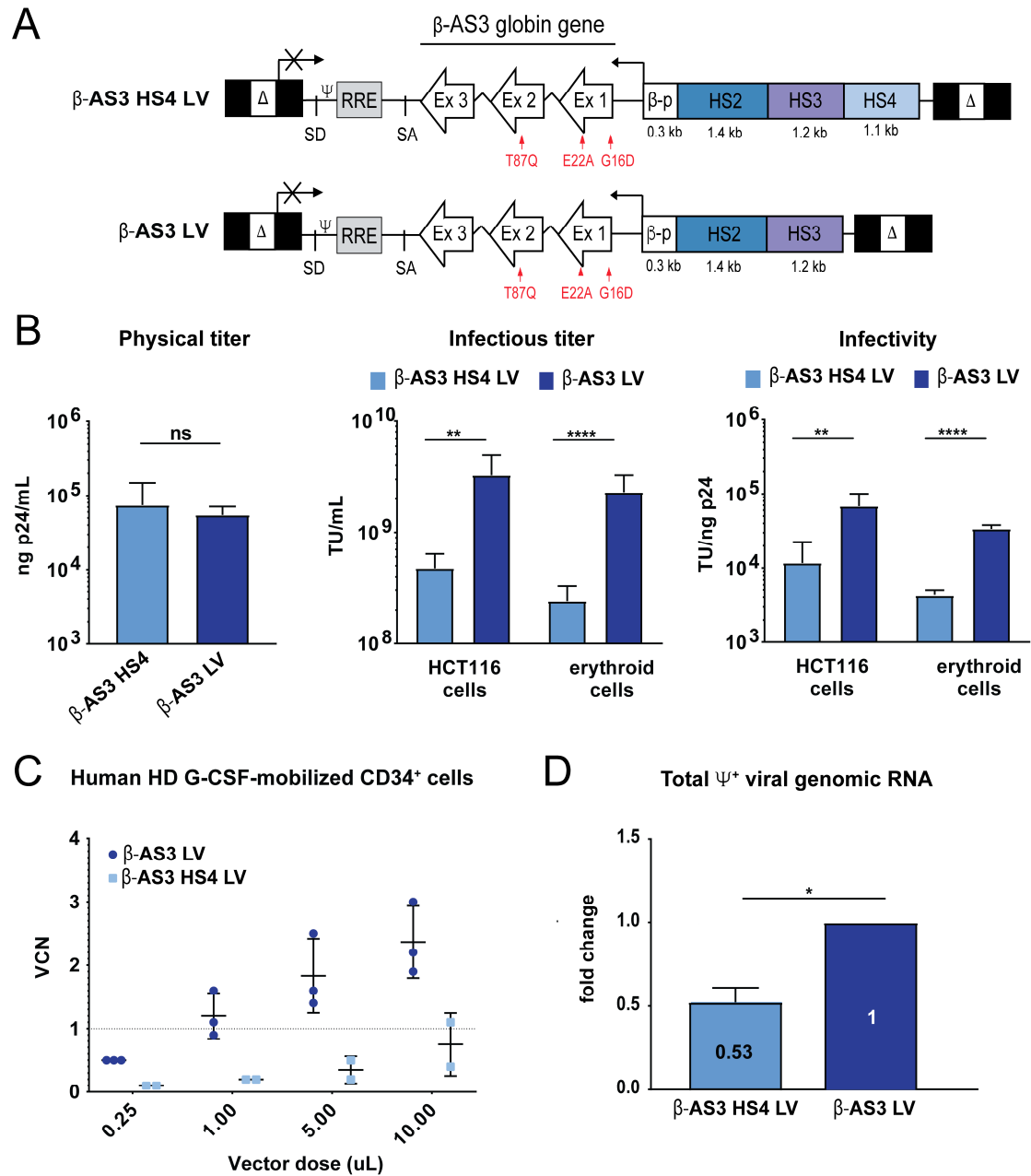


Figure 1

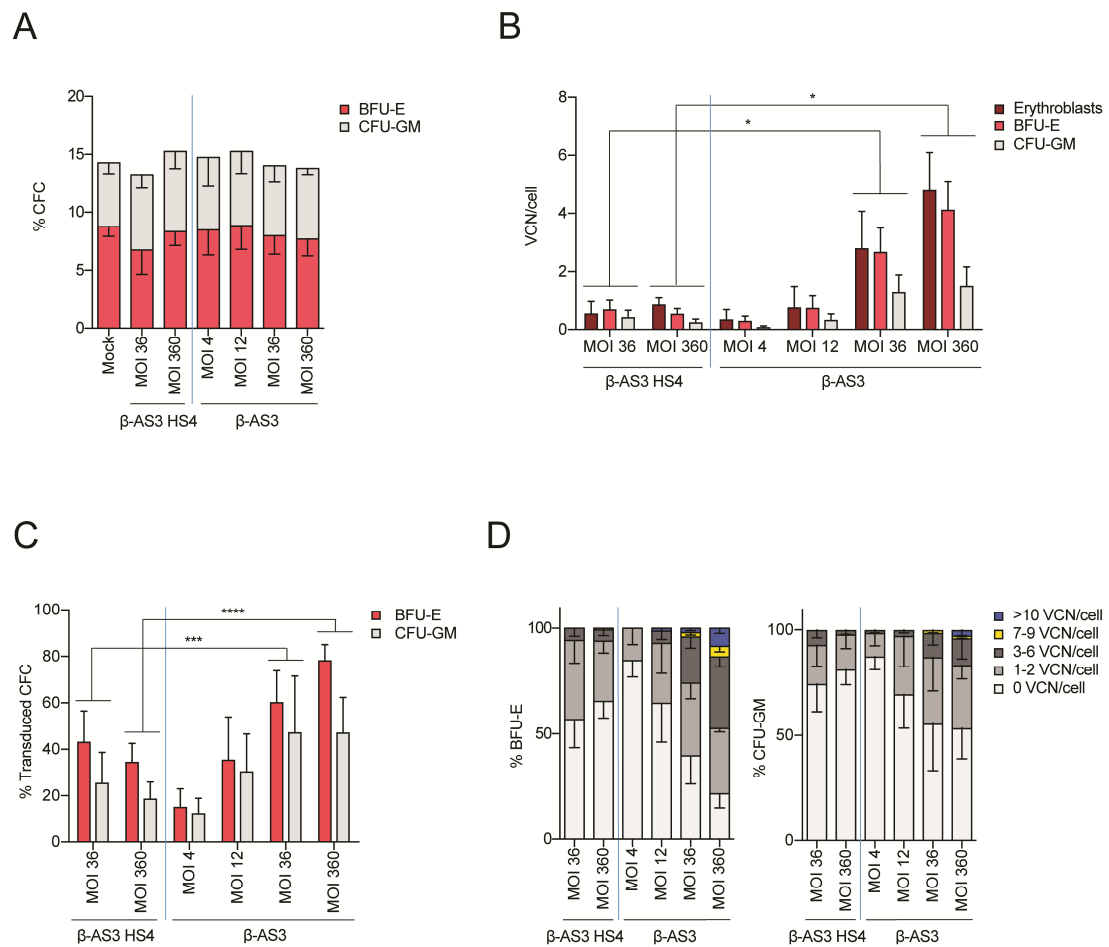


Figure 2



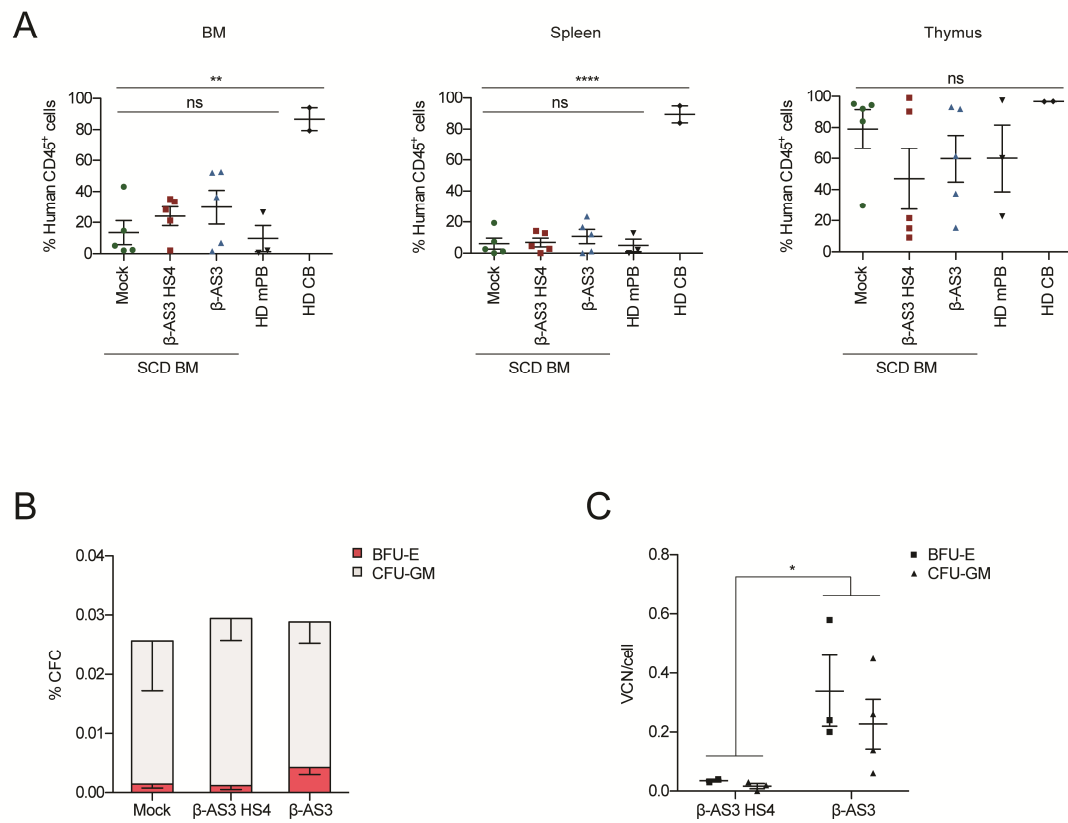


Figure 3

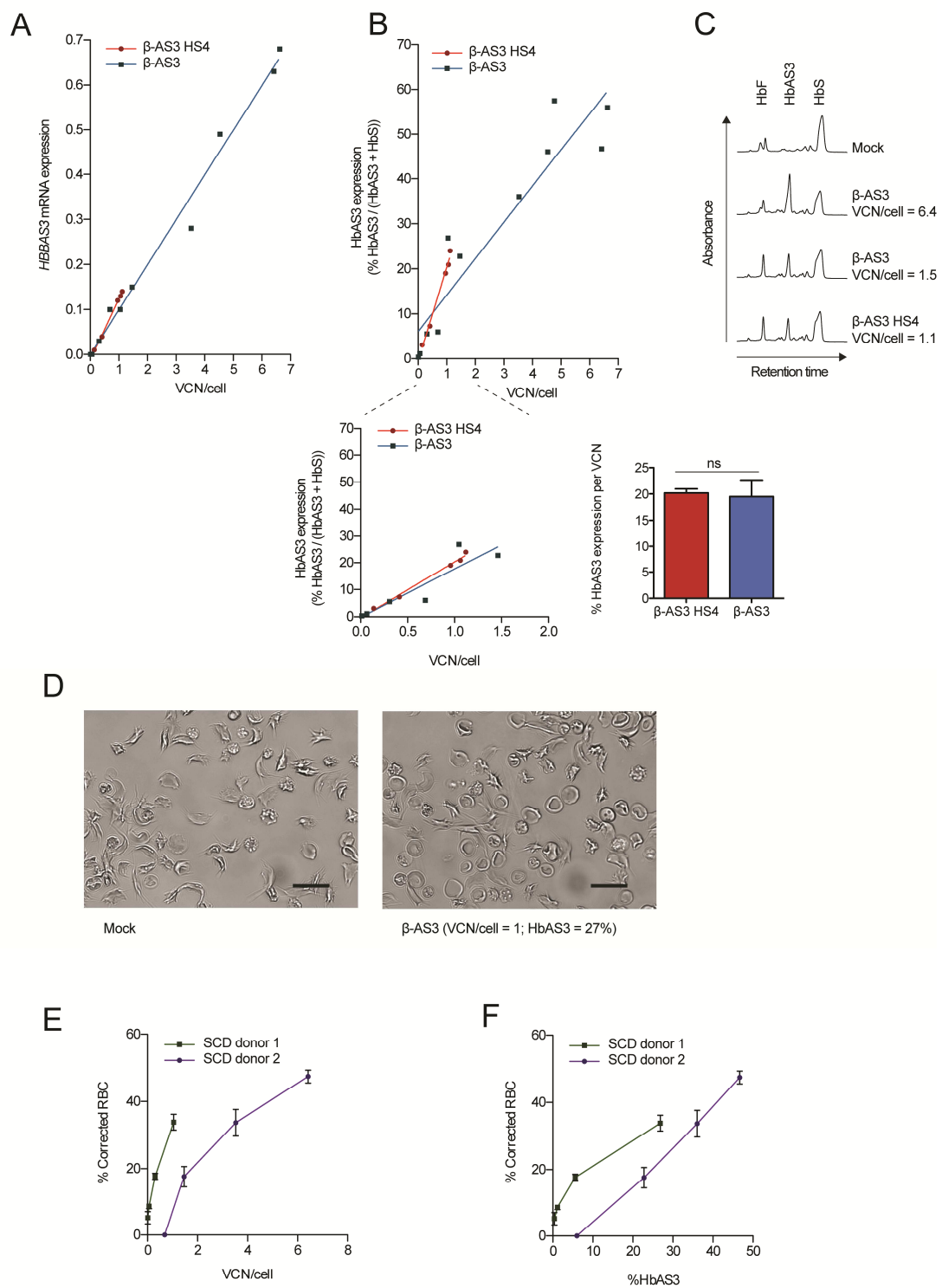


Figure 4

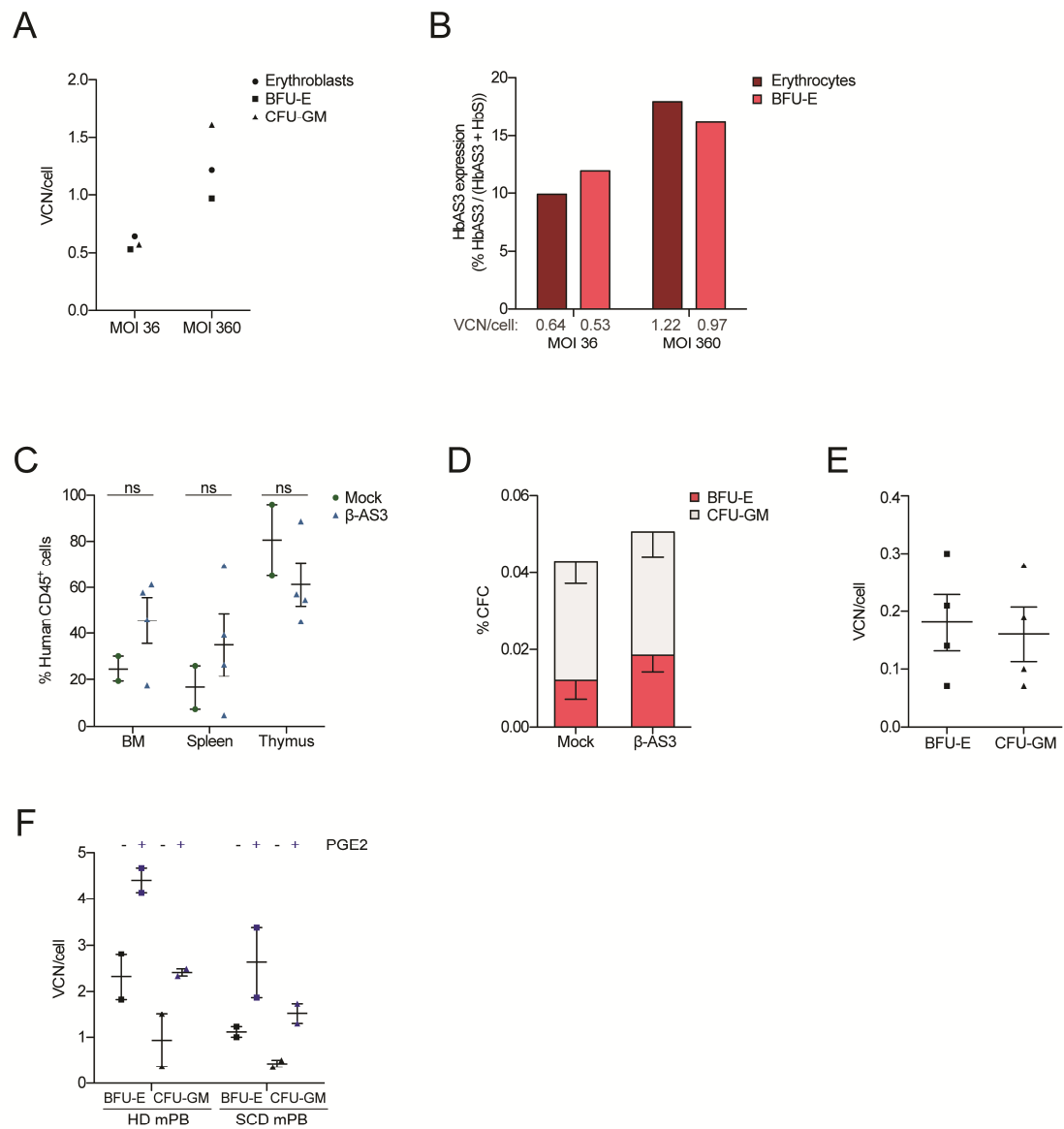


Figure 5